IL NUOVO CIMENTO Vol. 25 C, N. 5-6 Settembre-Dicembre 2002

High-resolution CCD spectra reduction: temporal changes of the flat-field compensation(*)

A. Kučera([1]), A. Hanslmeier([2]), J. Rybák([1]) and H. Wöhl([3])

([1]) *Astronomical Institute of the Slovak Academy of Sciences - 05960 Tatranská Lomnica Slovakia*
([2]) *Institut für Geophysik, Astrophysik und Meteorologie - Universitätsplatz 5, 8010 Graz Austria*
([3]) *Kiepenheuer-Institut für Sonnenphysik - Schöneckstr. 6, 79104 Freiburg, Germany*

(ricevuto il 10 Giugno 2002; approvato il 24 Settembre 2002)

Summary. — A new method suitable for long-time series of high-resolution CCD spectra reduction is presented. The method allows to compensate the temporal changes of the instrument conditions which leads to temporal changes of the flat-field matrix. Sometimes it is impossible to make the flat-field measurements during long simultaneous observations with satellites (SOHO, TRACE). The method splits the flat-field matrix into two components. The first one, connected with CCD camera is stable in time and is correct for all spectra. The second one varies and reflects temporal changes of the conditions in the spectrograph. Description of the method and its application to real high-resolution CCD spectra is presented and discussed.

PACS `95.55.Aq` – Charge-coupled devices, image detectors, and IR detector arrays.
PACS `01.30.Cc` – Conference proceedings.

1. – Introduction

The fundamental task of the photometric spectrum reduction is to "clean" the observed raw spectrum (see fig. 1a) without affecting the true spectral intensity information included in the image and to keep the S/N ratio as high as possible. The term "flat-field correction" then refers to the process of correction of the CCD image so that it acts as if it has a uniform response everywhere. But, the flat field is also used to take care of defects (reflections, dust, shutter effect, Newton's rings, etc.) in the optical system that result in non-uniform illumination of the chip. Therefore the flat field is absolutely essential for precise photometric analysis of CCD spectra.

(*) Paper presented at the International Meeting on THEMIS and the New Frontiers of Solar Atmosphere Dynamics, Rome, Italy, March 19-21, 2001.

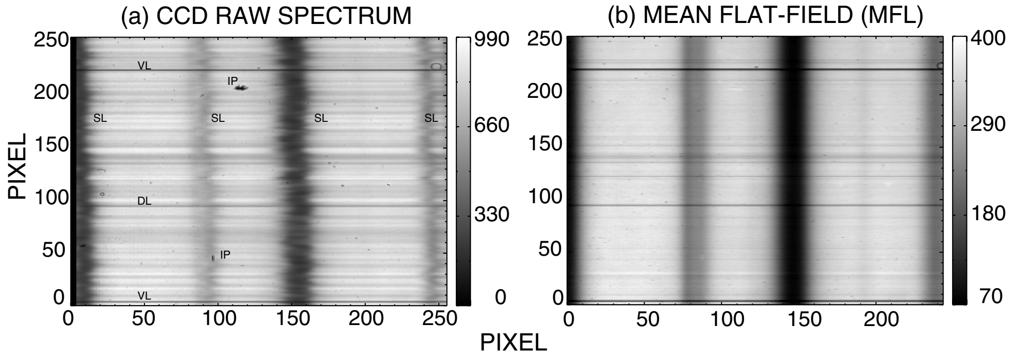

Fig. 1. – The CCD raw spectrum (a) and the cleaned $(\mathrm{MFL})_i$ (b). VL: the artificial wires put on the spectrograph slit; SL: spectral lines; DL: dust lines caused by dust particles laying on the slit; IP: imperfections come from wrong pixels of the CCD chip and/or from dust on the CCD camera window.

The aim of this paper is to demonstrate the reduction of solar CCD spectra taken in long-time series with short exposures with high spectral, spatial and time resolution. We will illustrate the reduction with the observations performed at the VTT, Tenerife, on September 7, 1996 using a 1024×1024 CCD camera. These spectra were taken at the VTT during a parallel campaign to SOHO/SUMER [1].

2. – Observations

The observing project mentioned included observations in four spectral regions with four CCD cameras simultaneously. The spectra were exposed with a high cadence of 5 seconds. Data were collected during several hours. Here, we will deal mainly with the observations of Fe I 649.4 nm line (eq. width = 165 mÅ, $g_{\mathrm{eff}} = 1.025$). A small area $7.6''$ wide near the disc center was scanned. Flat-field source frames (FF) and dark current frames (DC) were collected at the beginning and the end of the observing run. The width of the entrance slit of the spectrograph was $60\,\mu$m. The exposure time was 0.2 seconds. The binning mode was switched to 4×4, so the final spectrum has 256×256 pixels. Fe I 649.4 nm line was observed in the 35th order. Thus, one pixel corresponds to 8.4 mÅ and $0.35''$ in wavelength and spatial directions, respectively. One particular spectrum of the Fe I 649.4 nm line will be used here for a demonstration of the method.

3. – Spectra reduction

The reduction of the spectra was made using two different levels of precision.

Level A: the extended reduction consists of: a) DC, bias and parasitic light subtraction, b) flat-field source frame (FF) construction, c) cleaning of big defects (IP) from the spectrum, d) precise restoration of image inclination, e) restoration of the spectral line (SL) curvature and inclination, f) artificial horizontal lines (VL) excluding, g) flat fielding.

Level B: the precise reduction differs from the previous one in a special flat-field processing: h) splitting up the flat-field matrix into two matrices to eliminate long-term drift of the spectrograph and temporal changes of the flat-field conditions.

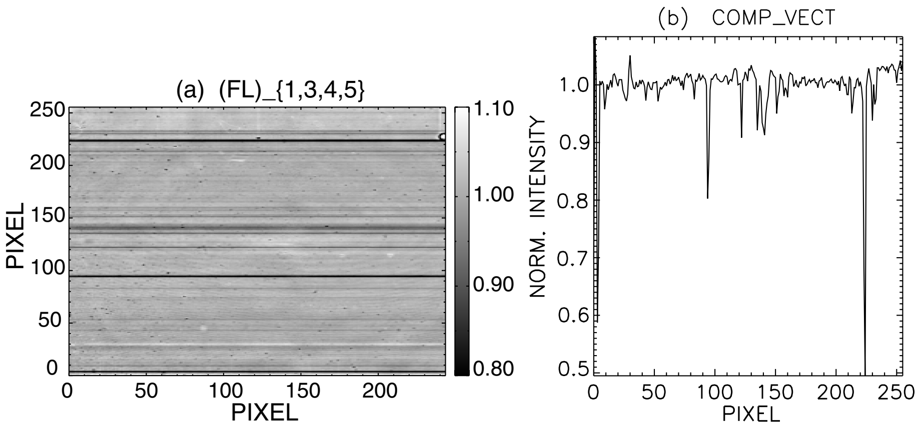

Fig. 2. – Flat-field correction matrix (a) and comp-vector (b).

We will concentrate on the description of the last two steps g) and h) to demonstrate the method which is necessary to use for reduction of the spectra taken in long-time series. Reduction is performed using programs written in Interactive Data Language (IDL).

3·1. *Level A—extended reduction.* – Let us start with the prepared "observed spectrum" SP and prepared "mean flat-field source" MFL (see fig. 1b). Both are already restored according to the steps a)-f). For flat fielding of the SP spectrum we can use the equation

$$\mathrm{RS} = \mathrm{SP} \prod_{i=1}^{n} \frac{1}{(\mathrm{FL})_i}\,, \tag{1}$$

where the RS is the reduced spectrum and flat field $(\mathrm{FL})_i$ is defined as

$$(\mathrm{FL})_i = \frac{(\mathrm{MFL})_i}{A_i}\,, \quad i = 1, 2, ...n, \tag{2}$$

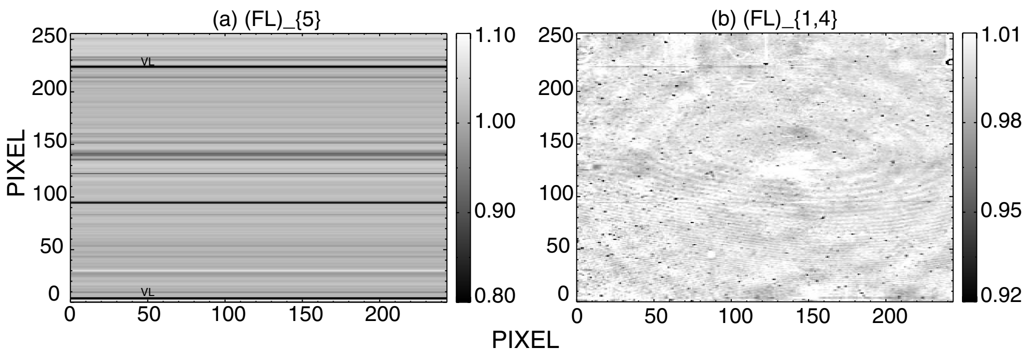

Fig. 3. – Spectrograph slit flat field (a) and CCD camera flat field (b).

where the mean flat-field source

$$(3) \qquad (\mathrm{MFL})_i = \frac{\sum_{k=1}^{K}[(\mathrm{FF})_k - \mathrm{MDC}]}{K}, \quad i = 1, 2, ...n.$$

K is the number of the flat-field source spectra frames FF taken with the moving telescope and the mean dark current

$$(4) \qquad \mathrm{MDC} = \frac{\sum_{l=1}^{L}(\mathrm{DC})_l}{L}$$

is an average of several particular DCs and bias images including the parasitic light of the spectrograph. Letter A denotes the average pixel value of the corrected flat-field source frame used for normalization, and i means the number of specific types of flat fields which take place in the particular reduction. The common types of flat fields we will deal with here are

$(\mathrm{FL})_1$ "pixel flat", the flat field used for the correction of the non-uniform sensitivity of the pixels across the chip.

$(\mathrm{FL})_2$ "illumination flat", the flat field which will correct large gliding changes of the intensity across the chip caused by for example optical vignetting, dust particles imaged out of the focus, etc.

$(\mathrm{FL})_3$ "shutter flat", the flat field used to suppress the non-uniformity of the exposure caused by the finite travel time of the shutter across the field of view.

$(\mathrm{FL})_4$ "camera flat", the flat field for correction of CCD camera effects, for example Newton's rings, or dust laying on the CCD camera window.

$(\mathrm{FL})_5$ "slit flat", the flat field for corrections of the non-uniform illumination of the chip caused by the dust laying on the spectrograph slit and/or by non-parallel edges of the slit.

Sometimes, several types of flat fields could be grouped into one flat-field source frame for correction of several effects together.

For computation of the denominators in eq. (1) we use IDL procedure "FLAT.PRO" from the KIS LIB IDL library (Kiepenheuer-Institut für Sonnenphysik, Freiburg). This gives directly $(\mathrm{FL})_{1,3,4,5}$ (see fig. 2a) and smoothed background $(\mathrm{FL})_2$ which represents the illumination flat field. Thus, we obtain the final equation for the *extended reduction* in the form

$$(5) \qquad \mathrm{RS} = \frac{\mathrm{SP}}{(\mathrm{FL})_2} \prod \frac{1}{(\mathrm{FL})_{1,3,4,5}},$$

the resulted spectrum RS from the extended reduction is demonstrated in fig. 4a.

There are still sharp horizontal lines and stripes in the RS. This is due to temporal changes of the flat-field conditions mainly caused by the drift of the spectrograph. Therefore, the mean flat-field source constructed from FFs taken at the beginning of the observing run does not match perfectly the flat-field conditions valid for the moment of the particular spectrum registration. The resulting flat field is slightly shifted in both directions comparing to the observed spectrum. Thus there are some defects enhanced instead of suppressed in the RS after this type of flat fielding.

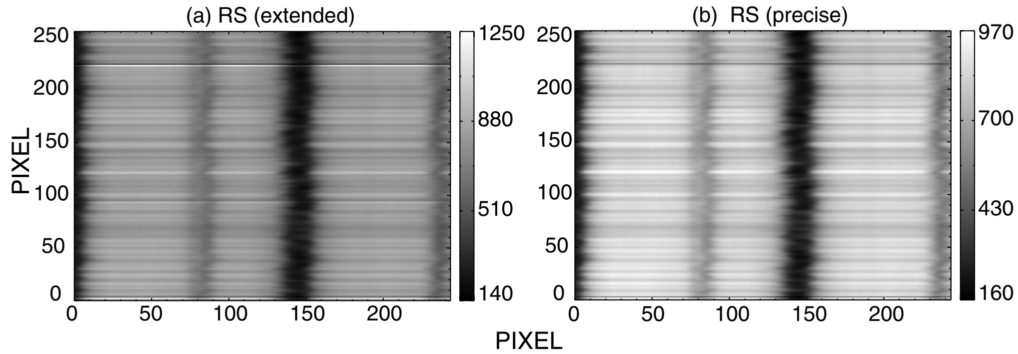

Fig. 4. – Resulted spectra from extended reduction (a) and precise reduction (b).

3˙2. *Level B—precise reduction.* – Long focal length spectrographs exhibit drifts of the spectral lines and changes of the dispersion, *e.g.*, due to thermal bending of mechanical components. The drift of the spectrum in the focal plane of the VTT spectrograph in both directions was found also in our data set. Values of 1.06 pm (1.3 pixel) per hour and 0.26 arcseconds (1.5 pixel) per hour were found for the X (spectral) and Y (spatial) direction, respectively. Movement of the spectrum in the focal plane of the spectrograph will affect mainly the $(\mathrm{FL})_5$, because the others are closely connected with CCD camera corpus or they are not sensitive to the movement. The slit-flat $(\mathrm{FL})_5$ shows rapid changes of the intensity across the camera field in Y direction seen as the horizontal white and black lines and stripes in the spectra. The movement of the slit-flat $(\mathrm{FL})_5$ in X direction is not important, because the horizontal lines do not change significantly their intensities in the X direction. But movement of the slit-flat $(\mathrm{FL})_5$ in Y direction even of a fraction of a pixel, changes dramatically the whole flat field $(\mathrm{FL})_i$, which then does not match the conditions valid for the SP. To solve this problem, we gain from the fact that only the slit-flat $(\mathrm{FL})_5$ is uniform in X direction. This is a direct consequence of the imaging of the slit in the focal plane of the spectrograph. Thus, the average of all columns of the $(\mathrm{FL})_{1,3,4,5}$ (let us call it "COMP-VECT", see fig. 2b) will mainly represent the intensity fluctuation of the $(\mathrm{FL})_5$ in Y direction, because: a) the intensities of the other two components, $(\mathrm{FL})_1$ and $(\mathrm{FL})_4$ are randomly distributed across the CCD image and they will not contribute systematically to the COMP-VECT. b) The third component $(\mathrm{FL})_3$ will be hidden in the COMP-VECT but due to its gliding character and small variations it will not support the rapid changes of the COMP-VECT in Y direction. So, if we will create new array of the same dimension as the $(\mathrm{FL})_i$ has and put the COMP-VECT to every column of the new array, we will immediately procure the slit-flat $(\mathrm{FL})_5$. Obtaining the $(\mathrm{FL})_5$ serves as a possibility to extract the $(\mathrm{FL})_{1,4}$ dividing the $(\mathrm{FL})_{1,3,4,5}$ by $(\mathrm{FL})_5$. The slit-flat $(\mathrm{FL})_5$ is represented in fig. 3a and $(\mathrm{FL})_{1,4}$ is shown in fig. 3b. The last steps in the *precise reduction* are then trivial. By comparing the Y positions of the VLs in $(\mathrm{FL})_5$ and in the spectrum, looking for the highest correlation, we estimate the difference and direction in which the slit-flat $(\mathrm{FL})_5$ must be shifted to match the spectrum SP. The new final $(\mathrm{FL})_{1,3,4,5}$, is composed of the shifted $(\mathrm{FL})_5$ and fixed $(\mathrm{FL})_{1,4}$. Dividing the spectrum SP by the new final $(\mathrm{FL})_{1,3,4,5}$ and by $(\mathrm{FL})_2$ gives the reduced spectrum RS which is shown in fig. 4b. We have computed spectral characteristics for every scan in both RS spectra resulted from *extended* and *precise* reduction. Other several manipulations were applied on the RSs beforehand to obtain the spectral characteristics:

a) true continuum intensities were calculated according to spectral atlas, b) Fast Fourier Transformation was used to smooth every particular spectral profile and c) zero position for line shifts measurement was calculated as a position of the center of the mean profile. The mean profile was constructed as an average of 412 profiles in RS which are situated between the VL wires.

The spectral characteristics, I_{c}—line continuum intensity, I_0—line center intensity, L_{sh}—line center shift, FWHM—full-width-at-half-maximum line intensity and EW—equivalent width were calculated with KIS LIB procedure ABS-PROF.PRO applied on every scan separately. We use the results followed from the *precise reduction* as a standard for errors estimation of the *extended reduction* approach.

4. – Discussion and conclusions

We have found that spectral characteristics computed from inaccurately reduced spectrum (fig. 4a) significantly differ from those computed from the correct spectrum (fig. 4b). Relative differences of the continuum intensities I_{c} are in the range of 3%, but frequently reached 5% and several times exceeded 10%. A similar situation is in the case of line center intensities I_0. Here the scatter of relative differences reached 4–5% and isolated values of 10% and more appeared. As a logical consequence of the erroneous values of I_{c} and I_0 also the FWHMs and EWs are incorrect. No significant changes were found for L_{sh}, which are less sensitive to an inaccuracy of the I_{c} and I_0.

Inaccurate r.m.s. values of I_{c} as well as of I_0 result from the incorrect spectrum. We have artificial shifted the slit-flat $(\mathrm{FL})_5$ from the correct position gradually with step of 0.1 pixel up to value of 3 pixels to test the influence of the effect of applying wrong flat-field matrix to spectrum SP. The correct value of the relative r.m.s. for I_{c} (0.048) changed gradually up to relative r.m.s. = 0.056 for the case of the 3 pixels shift. A similar situation exists for I_0.

Further development of the method and tests of the influences of incorrect reduction procedures on the spectral characteristic determination is in progress now.

* * *

This work was supported by GA SAV (grant VEGA 2/7229/20), by the international collaboration with the Austrian Academy of Sciences and by DFG grant 436 SLK 113/7/0-1. AH thanks the Austrian FWF (Proj. 13308) for financial support. The Vacuum Tower Telescope is operated by the Kiepenheuer-Institut für Sonnenphysik, Freiburg at the Observatório del Teide of the Instituto de Astrofísica de Canarias.

REFERENCES

[1] Curdt W., Kučera A., Rybák J., Schühle U. and Wöhl H., *ASP Conference Series*, **118** (1997) 322.